Biomedicine & Pharmacotherapy 177 (2024) 116822

Contents lists available at ScienceDirect

Biomedicine & Pharmacotherapy

journal homepage: www.elsevier.com/locate/biopha

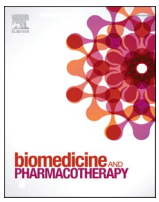

The Notch inhibitor, FLI-06, increases the chemosensitivity of head and neck Squamous cell carcinoma cells to taxanes-based treatment

Arkadiusz Czerwonka [a,*], Joanna Kałafut [a], Shaoxia Wang [b], Alinda Anameric [a], Alicja Przybyszewska-Podstawka [a], Mervi Toriseva [b], Matthias Nees [a]

[a] Department of Biochemistry and Molecular Biology, Medical University of Lublin, Lublin 20-093, Poland
[b] Institute of Biomedicine, Cancer Research Unit and FICAN West Cancer Centre Laboratory, University of Turku and Turku University Hospital, Turku, Finland

ARTICLE INFO

Keywords:
Notch signaling
Head and Neck Squamous Cell Carcinoma
FLI-06, Docetaxel
C-Jun

ABSTRACT

Aberration of Notch signaling is one of the key events involved in the development and progression of head and neck squamous cell carcinoma (HNSCC). The Notch pathway controls the tissue-specific differentiation of normal squamous epithelial cells and is frequently altered in squamous carcinomas, thus affecting their proliferation, growth, survival, and chemosensitivity or resistance against anti-cancer agents. In this study, we show that the use of novel, small-molecule inhibitors of Notch signaling, such as FLI-06, can have a beneficial effect on increasing the chemosensitivity of HNSCC to taxane-based chemotherapy. Inhibition of Notch signaling by FLI-06 alone virtually blocks the proliferation and growth of HNSCC cells in both 2D and 3D cultures and the zebrafish model, which is accompanied by down-regulation of key Notch target genes and proteins. Mechanistically, FLI-06 treatment causes cell cycle arrest in the G_1-phase and induction of apoptosis in HNSCC, which is accompanied by increased c-Jun^{S63} phosphorylation. Combining FLI-06 with Docetaxel shows a synergistic effect and partially blocks the cell growth of aggressive HNSCC cells via enhanced apoptosis and modification of c-Jun^{S243} phosphorylation via GSK-3β inhibition. In conclusion, inhibition of Notch signaling in HNSCC cells that retain active Notch signaling significantly supports taxane-based anticancer activities via modulation of both the GSK-3β and the c-Jun.

1. Introduction

Notch signaling controls processes such as lineage-specific differentiation, stemness, polarization and maturation of cells, and it is also tightly associated with diverse intracellular signaling pathways connected to proliferation, survival, and growth. Key elements of the Notch pathway are the four transmembrane NOTCH receptors (NOTCH1–4) and their ligands (Delta-like 1, 3 or 4 and Jagged 1 and 2). After activation, the NOTCH receptor undergoes a series of three proteolytic cleavages, finalized by the release and nuclear translocation of the NOTCH intracellular domain (NICD) after cleavage by the gamma-secretase complex. Once in the nucleus, the NICD acts as a part of an active transcriptional complex that regulates the expression of downstream NOTCH-responsive genes, including members of the HES and HEY family transcriptional regulator proteins, cyclin D1, cyclin-dependent kinase inhibitor 1 A (CDKN1A), and the c-MYC proto-oncogene [1].

Notch signaling controls the expression of key genes related to cell fate, proliferation, viability and chemoresistance. Consequently, aberrations in the Notch pathway are often associated with the progression of cancers, including head and neck squamous cell carcinoma (HNSCC) [2,3]. The oncogenic role of Notch signaling, mainly through gain-of-function (GoF) mutations and consequently, of hyper-activated Notch signaling, has been described in hematologic malignancies [4] and solid tumours such as triple-negative breast cancers [5]. In early-stage HNSCC, Notch receptors primarily act as tumor suppressors and are functionally inactivated by truncating, loss-of function (LoF) mutations. However, Notch signaling in advanced, recurrent and metastatic HNSCC is often activated or re-activated, by yet poorly understood mechanisms, including partial functional complementation between the four receptors [6,7]. Thus, Notch inhibition is considered a promising target for anti-cancer therapy in several cancer types, especially in advanced cancers. However, the presence of the four receptors, their unclear functional redundancy and complex tissue- and

* Corresponding author.
E-mail address: arkadiusz.czerwonka@umlub.pl (A. Czerwonka).

https://doi.org/10.1016/j.biopha.2024.116822
Received 24 March 2024; Received in revised form 21 May 2024; Accepted 26 May 2024
Available online 20 June 2024

cell-specific expression patterns, have confounded the research in this field. Furthermore, the most widely used inhibitors for targeting Notch signaling, the γ-secretase inhibitors, may block Notch signaling, but simultaneously affect over 140 additional targets of the γ-secretase complex and are therefore notoriously ambiguous and non-specific [8,9].

In previous studies, we have described the role of RIN-1, an activator of NOTCH signaling, in HNSCC [10]. In contrast, **FLI-06** is a pan-NOTCH receptor inhibitor that blocks maturation and secretion of all four NOTCH proteins prior to the release of the mature proteins from the endoplasmic reticulum [11]. There are several reports on the anticancer activity of **FLI-06** [11–14]. However, detailed mechanisms of action for **FLI-06** nor its potential effects specifically on HNSCC cancer cells have not yet been systematically investigated.

Taxanes (such as paclitaxel (PTX) and docetaxel (DTX)) are a group of effective anticancer compounds that act by stabilizing microtubule bundles, consequently preventing mitosis to proceed. Typically, cancer cells respond to taxane treatment by the arrest of the cell cycle in the G_2-M phase and inducing pro-apoptotic events [15]. However, additional anticancer mechanisms, for example, based on the inhibition of angiogenesis or ROS-mediated mechanisms, are also known [16]. NOTCH1-dependent resistance to taxanes has been reported in several cancer types, including breast [17,18], prostate [19,20], lung [21] and HNSCC [22,23]. Additionally, it was suggested that Notch signaling may be related to a unique resistance mechanism observed in HNSCC cells treated by taxanes [15]. It is speculated that inhibition of Notch signaling may be beneficial for taxane-based anticancer therapy. Thus, in the present study, we decided to evaluate the potential of the NOTCH pathway modulator **FLI-06**, to improve taxane-based anti-HNSCC therapy.

C-Jun, together with c-Fos a component of the dimeric transcription factor activator protein-1 (AP-1), is a key protein for activating the transcription of genes that regulate cell growth, differentiation and survival [24] especially in (squamous) epithelial cells, and keratinocytes [25]. Activation of c-Jun plays also a key role for mitochondrial cytochrome c release, caspase activation, and consequently apoptotic cell death [26,27]. The activity and stability of c-Jun is strictly related to its phosphorylation state. It is know that C-Jun^{S63} phosphorylation increases the transcriptional potential and stability of c-Jun as a part of the AP-1 complex [28]. In contrast, c-Jun phosphorylation at serine 243 (c-Jun^{243}) by active GSK-3β keeps c-Jun in a non-binding state, inactive [29].

2. Materials and methods

2.1. Cell lines and cell culture conditions

The University of Turku Squamous Cell Carcinoma (UT-SCC) cell lines panel 1. UT-SCC-24A - tongue squamous cell carcinoma; 2. UT-SCC-24B - tongue squamous cell carcinoma, derived from the metastatic site of the same patient (cervical lymph node), 3. UT-SCC-42A - laryngeal squamous cell carcinoma; 4. UT-SCC-42B - laryngeal squamous cell carcinoma, derived from metastatic site of the same patient (cervical lymph node), 5. UT-SCC-38 - laryngeal squamous cell carcinoma, 6. UT-SCC-44 - gingival squamous cell carcinoma, and 7. UT-SCC-60A - tonsillar squamous cell carcinoma) were established and obtained from Turku University Central Hospital, Finland. 8. HNSCC SSC-9 (CRL-1629; Human tongue squamous cell carcinoma) and 9. SCC-25 (CRL-1628; Human tongue squamous cell carcinoma) cell lines were obtained from ATCC (Rockville, Maryland USA). Cells were cultured in DMEM-F12 (Sigma-Aldrich) medium supplemented with 10 % FBS and penicillin (100 units/ml) / streptomycin (100 μg/ml) at standard culturing condition (37℃, 5 % CO_2). The proper cell density was estimated by automated cell counting on a TC20™ (Bio-Rad) cell counter before each experiment. Cells were harvested (5 mM EDTA in PBS without Ca^{2+} and Mg^{2+}) and centrifuged (500 g) for further analysis.

2.2. Drugs and chemical reagents

FLI-06 (cyclohexyl 2,7,7-trimethyl-4-(4-nitrophenyl)-5-oxo-1,4,5,6,7,8-hexahydroquinoline-3-carboxylate), CB-103 (6-(4-Tert-butylphenoxy)pyridin-3-amine)), RIN-1 (2-(2-Fluorophenoxy)-4-(1-methyl-1 H-pyrazol-5-yl)benzamide)) were purchased from Selleck Chemicals GmbH (Munich, Germany). DAPT [N-[N-(3,5-Difluorophenacetyl)-L-alanyl]-S-phenyl-glycine t-butyl ester], and Docetaxel (DTX; N-Debenzoyl-N-(tert-butoxycarbonyl)-10-deacetyltaxol) were purchased from Merck (Darmstadt, Germany). Compounds' Stock solutions were prepared in DMSO according to the manufacturer's instruction and stored at −80℃. All other chemical reagents were obtained from Merck (Darmstadt, Germany) unless indicated differently.

2.3. Cell viability, proliferation and growth assays in 2D and 3D condition

The cell proliferation analyses in 2D culture condition were performed with MTT assay. In brief, cells were seeded onto a 96-well plate at a density of 3–5 × 10^4 cells/ml. After cells attached (24 h), the culture medium was removed, and the cells were exposed to serial dilutions of the tested drugs. After 96 hours, cells were exposed to MTT (3-(4,5-dimethylthiazol-2-yl)-2,5-diphenyltetrazolium bromide, 15 μL, 5 mg/ml in PBS, 3 h of incubation). Formed formazan crystals were solubilized by adding SDS buffer (10 % SDS in 0.01 N HCl, overnight incubation), and absorbance was determined at a wavelength of 570 nm using an M200 Pro microplate reader (Tecan). Proliferation inhibition results (mean ± SD) were calculated as % of control (absorbance values of untreated cells).

For viability assay, the CyQUANT™ LDH Cytotoxicity Assay kit (Thermo Fisher) was used. UT-SCC-42B cells were seeded on 96-well plates (5 × 10^5 cells/ml; 100 μl of full culture medium). After 24 hours, the cells were exposed to a range of FLI-06 concentrations (medium supplemented with 2 % FBS). Next, the supernatants were collected after 24 and 48 hours. The LDH levels released into the medium were measured according to the manufacturer's instructions. Absorbance was determined at a wavelength of 570 nm using an M200 Pro microplate reader (Tecan). LDH levels in supernatant (mean ± SD) were calculated as % of control (absorbance values of untreated cells).

For the impact of **FLI-06** on cell proliferation in 3D condition, the "3D sandwich model" described previously [30] was used. In brief, UT-SCC cells in Matrigel Basement Membrane Matrix (Corning) were seeded in 96-well angiogenesis μ-slides plate. Next, single freshly seeded UT-SCC cells were immediately treated with medium containing the appropriate concentration of drug (impact of **FLI-06** on cell survival and initial formation of organoids when transferred to Matrigel). Alternatively, the cells were left to grow and form organoids in Matrigel for 3 days before they were exposed to the drug (impact of **FLI-06** on growth and proliferation of mature organoids). Growth of UT-SCC organoids were observed by real-time visualization in IncuCyte live-cell imager (Essen Bioscience). Analysis of obtained UT-SCC photos and calculation of the average size of organoids (mean ± SD; $μm^2$) was performed by using Incucyte Base Analysis software.

2.4. Relative mRNA expression, Western blot, and immunofluorescence staining

The total RNA was extracted using RNeasy kit (QIAGEN) according to the manufacturers protocol. The cDNA synthesis was performed through High-Capacity cDNA Reverse Transcription Kit (Applied Biosystems). The qPCR analysis was performed with the LightCycler® 480 II instrument (Roche) using PowerUp SYBR Green Master Mix (Applied Biosystems) protocol and 25 ng of cDNA on each reaction. The following primer sequences were used:

GAPDH (forward 5'-GTGGAGTCTACTGGTGTCTTC-3', reverse 3'-

GTGCAGGAGGCATTGCTTACA-5'),

HES1 (forward 5′-TCAACACGACACCGGATAAAC-3′ and reverse 3′-GCCGCGAGCTATCTTTCTTCA-5′),

HEY1 (forward 5′-CGGCTCTAGGTTCCATGTCC-3′ and reverse 3′-GCTTAGCAGATCCCTGCTTCT-5′),

NOTCH1 (forward 5'-CAACTGCCAGAACCTTGTGC-3' and reverse 3′-GGCAACGTCAACACCTTGTC-5′),

NOTCH2 (forward 5′-GGCACGTCAGGGGTTAATTG-3′ and reverse 3′-GCGGAAACCATTCACACCGTTGAT-5′),

NOTCH3 (forward 5′-GCAGATGGCTCAACGGCACTG-3′ and reverse 3′-GGGGTCTCCTCCTTGCTATCCTG-5′),

JAG1 (forward 5′-GCCGAGGTCCTATACGTTGC-3′ and reverse 3′-CCGAGTGAGAAGCCTTTTCAA-5′),

DLL1 (forward 5′-TGCCTGGATGTGATGAGCAGCA-3′ and reverse 3′-ACAGCCTGGATAGCGGATACAC-5′),

CCNA2 (forward 5′-CTCTACACAGTCACGGGACAAAG-3′ and reverse 3′-CTGTGGTGCTTTGAGGTAGGTC-5′),

CCNB1 (forward 5′-GACCTGTGTCAGGCTTTCTCTG-3′ and reverse 3′-GGTATTTTGGTCTGACTGCTTGC-5′),

CCNE1 (forward 5′-TGTGTCCTGGATGTTGACTGCC-3′ and reverse 3′-CTCTATGTCGCACCACTGATACC-5′),

CCND1 (forward 5′-TCTACACCGACAACTCCATCCG-3′ and reverse 3′-TCTGGCATTTTGGAGAGGAAGTG-5′).

CDKN1A (forward 5′-AGGTGGACCTGGAGACTCTCAG-3′ and reverse 3′-TCCTCTTGGAGAAGATCAGCCG-5′),

CDKN1B (forward 5′-ATAAGGAAGCGACCTGCAACCG-3′ and reverse 3′-TTCTTGGGCGTCTGCTCCACAG-5′),

Relative mRNA expression was calculated using the $2^{-\Delta\Delta Ct}$ subtraction method and normalized to the expression of the *GAPDH* housekeeping gene. The fold change (FC) of target gene expression in the range of 0–0.749 was considered as downregulated; no change for 0.75–1.5; and upregulated for a FC between 1.501 and 5, respectively.

For Western blotting and phospho-kinase array assays, protein lysates were obtained by lysing cells with RIPA Buffer (Thermo Scientific). Next, protein concentration was quantitated by using Pierce BCA Protein Assay Kit (Thermo scientific). To assess protein expression, standard SDS-PAGE polyacrylamide gel electrophoresis and Western blotting, based on the Bio-Rad Western Blotting Protocols (Bio-Rad), were performed. The primary antibodies were used: rabbit NOTCH1/NICD1 (D1E11 XP(R); Cell Signaling, Beverly, MA, USA), NOTCH3/NICD3 (D11B8; Cell Signaling), HES1 (D6P2U; Cell Signaling), HES5 (EPR15578; Cambridge, MA, USA), c-Jun (60A8; Cell Signaling), Phospho-c-Jun (Ser63) (E6I7P, Cell Signaling), Phospho-c-Jun (Ser243) (Cell Signaling), and BAX (D2E11; Cell Signaling). β-actin (C4 mouse monoclonal IgG1; Santa Cruz Biotechnology, and rabbit (13E5); Cell Signaling)) were used as house-keeping gene. The secondary antibodies used were: anti-rabbit-IR800 (Li-Cor Biosciences, Lincoln, NE), anti-mouse IgG (H+L) (DyLightTM 680 conjugate; Cell Signaling), and anti-rabbit IgG, HRP-linked (Cell Signaling) antibodies. The membranes were imaged with the Li-COR Odyssey Infrared Imaging System. Proteome Profiler Human Phospho-Kinase Array Kit (Cat. Numb. ARY003C; Bio-Techne/R&D Systems) was used to evaluate changes in protein phosphorylation levels. Densitometric analysis was pperformed using the ImageJ-Fiji software.

For immunofluorescence (IF) staining, the UT-SCC-42A cells were fixed with 3 % paraformaldehyde and blocked with 3 % bovine serum albumin (in PBS). Next, cells were labeled with anti-NOTCH1 antibody, anti-E-cadherin, and anti-F-actin antibody (R&D Systems, Minneapolis, MN). Alexa Fluor 633 donkey anti-goat IgG (H+L), Alexa Fluor 568 goat anti-rabbit IgG (H+L) and Alexa Fluor 488 donkey anti-sheep IgG (H+L) (Invitrogen, Carlsbad, CA) were used as secondary antibodies. The cells were mounted in Mowiol-DABCO (Sigma-Aldrich) and examined with Zeiss LSM510 META confocal microscope (Carl Zeiss, Jena, Germany).

2.5. Cell cycle and induction of apoptosis

The HNSCC cells were seeded into 6-well microplates at a density of 5×10^5 cells/ml. After 24 h, the cells were exposed to a range of drugs concentrations and incubated for 48 h. After harvest, cell were centrifuged and fixed with 70 % ice-cold ethanol and stored at − 20 °C. PI/RNase (PI/RNase Staining Buffer, BD Pharmingen, Catalogue Number 550825, Franklin Lakes, New Jersey, U.S.) staining was performed directly before the flow cytometric analysis (BD FACSCalibur, CellQuest Pro Version 6.0. software for the Macintosh operating system.). The PI fluorescence intensity of individual nuclei was determined and at least 10000 events an acquisition rate of 100–300 events/s.

For both Annexin V/Propidium iodide (PI) and active caspase-3 assays, cells were prepared as described above. After detaching, cells were centrifuged (500×g), washed in PBS, and further analyzed in a BD FACSCalibur flow cytometer. The number of apoptotic and necrotic cells was measured with the FITC Annexin V Apoptosis Detection Kit I (BD Pharmingen). Additionally, the activation of caspase-3 was measured by PE Active Caspase-3 Apoptosis Kit (BD Pharmingen). Both assays were performed according to the manufacturer's instructions.

2.6. Evaluation of FLI-06 and DTX drug combination against HNSCC

The antiproliferative effect of each drug combination was analyzed using SynergyFinder 3.0 [31] software. Inhibition of proliferation by appropriate combinations of the tested drugs was assessed by MTT assay as previously described (chapter 2.3). Next, results of combined FLI-06 and DTX treatment were evaluated by comparing differential responses to drug combinations with a reference mathematical model (the high single agent (HSA) model, according to the software recommendation). The summary synergy score (SSS; average excess response due to drug interactions), 3D synergy maps (synergistic and antagonistic regions in red and green colors, respectively), and the most synergistic area (MSA; the most synergistic 3-by-3 dose-window in a dose-response matrix) for a tested drugs were obtained automatically by SynergyFinder 3.0. All detailed results of analysis are presented in the supplemental materials. The FLI-06/DTX interaction was described as: synergistic (synergy score > 10) / additive (synergy score range between 10 and 0) (combination effect is higher than expected) or antagonistic (synergy score < 0; combination effect is lower than expected).

2.7. Zebrafish xenograft experiments

The zebrafish xenograft experiments were performed as previously described [10]. In brief, zebrafish (*Danio rerio*) strains used in the present study were obtained from the Experimental Medicine Center at the Medical University of Lublin. Adult zebrafish were raised at 28.5 °C under 14 h of light and 10 h of the dark cycle. Embryos were maintained in the E3 buffer. The FLI-06 and DTX drug toxicity assay in zebrafish was performed according to Ali et al. [32]. Vybrant DiD (Invitrogen) stained SCC-9 cells were cultured, implanted in the 2 days post fertilization (dpf) zebrafish embryos, and observed by using an EVOS M5000 Imaging System. Xenografts areas were quantified with the Fiji (ImageJ) software.

For qPCR analysis, total RNA from fish was isolated according to procedure described above (see chapter *2.4*). Zebrafish β-actin (*bact*: forward 5'-CATCCATCGTCCACAGGAAGTG-3', revers 5'-TGGTCGTTCGTTTGAATCTCAT-3') was used as a housekeeping gene. The human *GAPDH* gene (forward 5'-CTCTGCTCCTCCTGTTCGAC-3', revers 5'-GCCCAATACGACCAAATCC-3') was used to quantify the number of human cells in the injected zebrafish larvae in 5th dpf. The human *BAX* (forward 5′-TCAGGATGCGTCCACCAAGAAG-3′ and reverse 3′-TGTGTCCACGGCGGCAATCATC-5′) and *CDKN1A* (forward 5′-AGGTGGACCTGGAGACTCTCAG-3′ and reverse 3′-TCCTCTTGGAGAAGATCAGCCG-5′) were used to quantify the level of human *BAX* and *CDKN1A* mRNA with human *GAPDH* as a housekeeping gene. All

experiments were approved by the Medical University of Lublin's Animal Research Ethics Committee.

2.8. Statistical analysis and preparation of graphs

Statistical analyses were performed by using GraphPad Prism 8.0 (GraphPad Software Inc., California, U.S.A). One-way ANOVA followed by Tukey's posthoc test and column statistics were used for comparisons (*p ≤ 0.05; **p ≤ 0.01; ***p ≤ 0.001 ****p ≤ 0.0001 was considered statistically significant). All tests were performed in triplicates, at least. Biorender, Inkscape, and ImageJ-Fiji software were used to prepare the figures.

3. Results

3.1. Effect of FLI-06 on HNSCC proliferation, viability and growth under 2D and 3D culture conditions

Firstly, we assessed the antiproliferative activity of the inhibitor **FLI-06** in 2D culture conditions, using our representative panel of HNSCC cell lines by MTT assay. The analysis showed that the cells displayed a dose-dependent chemosensitivity against **FLI-06** (Fig. 1A). The most pronounced effects were observed for SCC-9 and SCC-25 cell lines, for which the IC_{50} value was estimated at 1.93 and 3.81 μM, respectively. Less pronounced efficacy (IC_{50} between 10 and 20 μM) was observed for the UT-SCC panel of cell lines (Table 1, Supplementary material). Additionally, to evaluate the potential impact of **FLI-06** on HNSCC viability and non-specific cytotoxicity, the LDH release assay was performed. Disruption of the cell membrane, and increased levels of LDH release was only observed for relative high concentrations of **FLI-06** between 25 and 50 μM, and only after 48 hours of prolonged drug exposure (Fig. 1B). No significant increase in LDH release was observed for **FLI-06** after 24 hours of drug exposure for concentrations < 15 μM. Considering these data, we conclude that the reduction of HNSCC cell proliferation in a concentration range up to 10 μM of **FLI-06** is restricted to the specific effect of **FLI-06** on inhibition of Notch signaling, rather than non-specific and cytotoxic off-target effects that may result in damage to the cell membranes.

Next, to indicate the impact of **FLI-06** on cell proliferation versus differentiation/maturation of developing tumour organoids in 3D condition, the "3D sandwich model" assay was performed. The HNSCC cells were seeded in laminin-rich, differentiation-promoting Matrigel matrix and observed in real-time, live cell culture conditions using the IncuCyte imaging system. When embedded in Matrigel, single HNSCC cells generated well-formed, round, and dense multicellular organoids (Ctrl; Fig. 1C;E) over a period of 3–4 days, which then continue to grow larger. When added early (at day 1, simultaneous to seeding) to cell cultures, even the lowest concentration of **FLI-06** (5 μM) completely prevented the formation of organoids (Fig. 1C; D) from single cells embedded in Matrigel. When added at a later time point (3 days-old organoids), **FLI-06** immediately reduced the growth of organoids that had already formed in Matrigel (Fig. 1E; F), and no growth was observed after 1 day treatment.

To further validate the specific effects of **FLI-06** as an inhibitor of Notch signaling in HNSCC, a series of qPCR and Western blots experiments were performed. After 72-h incubation of UT-SCC-42B cells with 2.5 μM **FLI-06**, a significant decrease in mRNA expression for key Notch signaling molecules such as *NOTCH1*, *NOTCH3*, *JAG1* and *DLL1* and NOTCH target genes, such as *HES1* and *HEY1* (Fig. 1G) was observed. The potential of **FLI-06** to inhibit Notch signaling was also confirmed at the level of protein expression. The Western blot analysis revealed that both 48- and 72- hours treatment of HNSCC cells with **FLI-06** resulted in significantly decreased expression levels of HES1 and HES5 at 6 and 10 μM. Additionally, an increase in FL-NOTCH1 (full length) expression and a simultaneous decrease in NICD1 (cleaved NOTCH1) and NICD3 (cleaved NOTCH3) in HNSCC cells was observed (Fig. 1H).

To visualize the impact of **FLI-06** on the localization of NOTCH1 protein, immunofluorescence staining (IF) on fixed cells was performed. As expected, HNSCC cells treated with **FLI-06** showed an accumulation of NOTCH1 protein in the cytoplasm but exclusion from the nucleus; a clear indication of interruption of active NOTCH signaling in treated cells. An increase in FL-NOTCH1 expression supports the information about **FLI-06**-dependent accumulation of NOTCH receptors in the cytoplasm, which was suggested by Krämer et al., [11]. Additionally, compared to untreated cells, a lower intensity level of F-actin microfilament arrangements (cortical actin underneath the plasma membrane) and dissociation of membrane-associated E-cadherin was observed after **FLI-06** treatment (Fig. 1I). In conclusion, **FLI-06** exhibits anticancer properties in both 2D and 3D culture conditions, affecting cells proliferation, growth and formation of HNSCC organoids, and effective inhibits Notch signaling in HNSCC cells.

3.2. Evaluation of the antitumor activity of FLI-06 and DTX in the context of Notch signaling activity in the HNSCC model

Similarly to **FLI-06**, we also assessed the anti-proliferative activity of the **DTX** in 2D culture condition. All HNSCC cell lines tested indicate relatively high, dose-dependent chemosensitivity against **DTX** (Fig. 2A), resulting in IC_{50} values in the range of 0.64 – 1.71 nM (Table1, Supplementary material). Next, to assess antiproliferative potential of various **FLI-06** and **DTX** combinations against HNSCC, multi-drug combination response tool (SynergyFinder 3.0 software) was used. Firstly, the antiproliferative potential of various combinations of **FLI-06** and **DTX** were tested against four HNSCC cell lines by MTT assay (UT-SCC-24A, UT-SCC-24B, SCC-9, and SCC-25). According to bioinformatic analyses of previously published data [33], all of these cell lines expressed NOTCH receptors 1–4, were devoid of truncating LoF mutations in these genes, and also expressed all or most of the Notch ligands. The most pronounced, additive effect was seen for the SCC-9 cell line (SSS = 4.81; MSA = 6.98) followed by UT-SCC-24A (SSS = 3.26; MSA = 5.2). Additionally, an additive effect **FLI-06** and **DTX** combinations on inhibition of cell proliferation was also observed for other HNSCC cell lines (Fig. 2B; C). To verify the additive effect of Notch signaling inhibition and taxane combination in HNSCC cells, additional Notch signaling inhibitors such as **CB-103** and **DAPT** were tested in combination with docetaxel. Also in these cases, additive interactions between Notch signaling inhibitors and **DTX** were observed (Fig. 2C). Finally, we also decided to use a Notch signaling activator, **RIN-1** [10]. In this case, **RIN-1** indicated mild additive (UT-SCC-24B), lack (SCC-9) or antagonistic (SCC-25, and UT-SCC-24A) interaction with **DTX** (Fig. 2C), thus illustrating that biochemical activation of NOTCH signaling has opposing effects when compared to inhibition.

Next, based on mRNA gene expression data from a panel of HNSCC-derived cell lines [33], we selected cell lines representing high (UT-SCC-44), medium (UT-SCC-38), and low level (UT-SCC-60A) Notch activity, as suggested by differential Notch signature [34], analyzed by gene set enrichment analysis (GSEA). Further proliferation assays revealed that the tested cell lines indicate a positive correlation between high Notch signaling signature and chemoresistance to **DTX** (Fig. 2D), with IC_{50} values 0.9, 0.64 and 0.54 nM for UT-SCC-44, UT-SCC-38, and UT-SCC-60A, respectively (Table 1, Supplementary material). Surprisingly, no relationship between the Notch signature of the tested HNSCC cell lines, and sensitivity to **FLI-06** was observed (Fig. 2E). However, as with the previously tested HNSCC cell lines, an additive effect of the combination of both drugs was observed for cell lines UT-SCC-44, UT-SCC-38, and UT-SCC-60A (Fig. 2F). In addition, the anti-proliferative potential of **FLI-06** and **DTX** drug combinations showed a positive correlation between high Notch signature and effectiveness of co-treatment. MSA score 13.5 and 10.6 for UT-SCC-44 and UT-SCC-38, respectively indicate synergistic type of interaction between tested drugs for high and, medium Notch signaling signature cells. An MSA score of 6.82, indicating an additive type of interaction, was

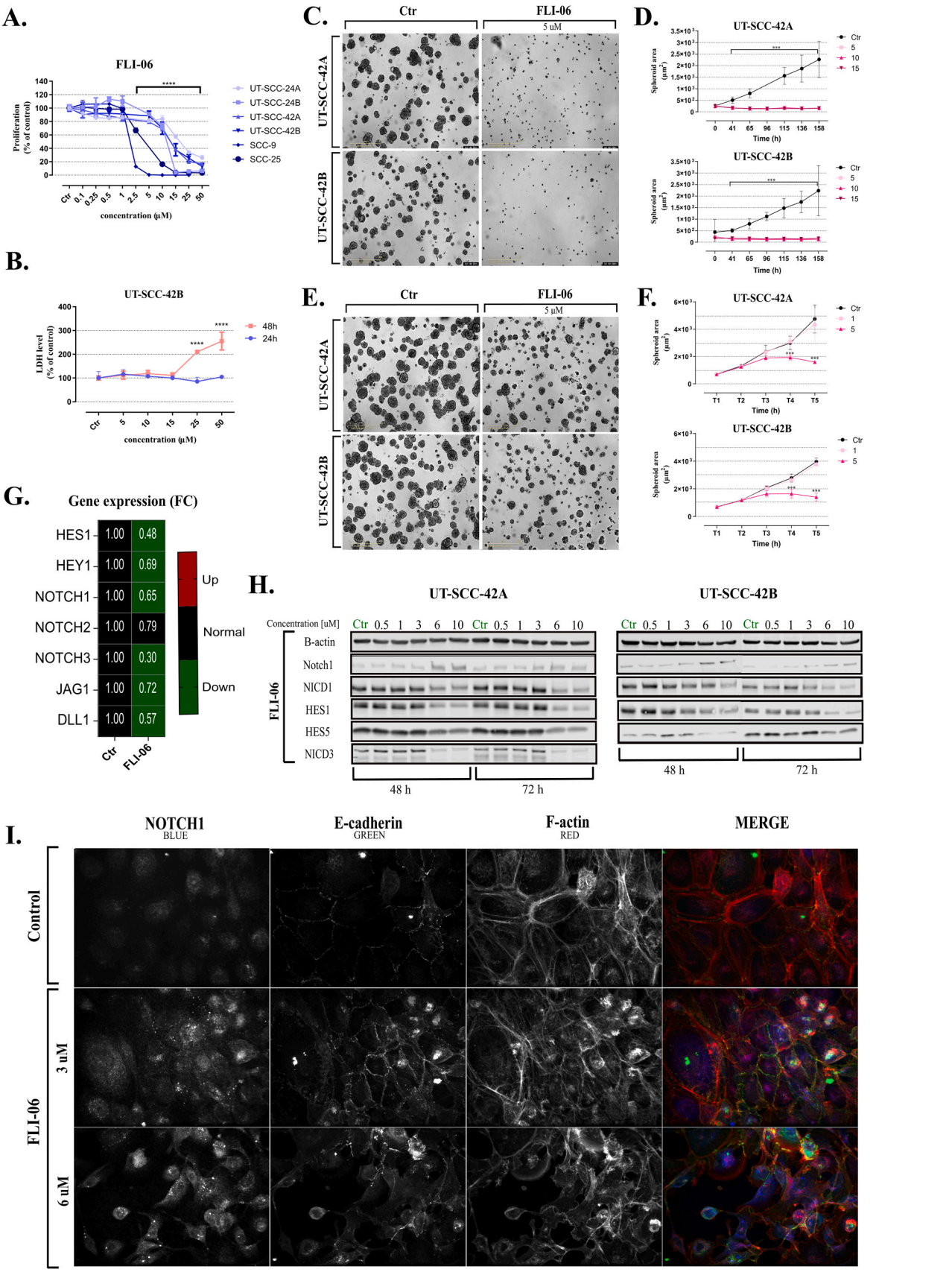

(caption on next page)

Fig. 1. The effects of FLI-06 on proliferation, cytotoxicity, and growth of HNSCC cell lines. (A) Cancer cell proliferation (% of control) at the endpoint of experiments (96 h) assessed by MTT assay. (B) The influence of FLI-06 on the permeability of UT-SCC-42B cells measured after 24 and 48 hours of drug exposure by lactate dehydrogenase (LDH) release assay. (C) Impact of FLI-06 on proliferation of UT-SCC-42A and 42B in 3D cultures. Representative photos of single HNSCC cells seeded simultaneously with FLI-06 exposure. (D) Average size of organoids (mean ± SD; μm^2) over time from treatment of single cells as measured by automated image analysis. (E) Treatment of mature organoids (3 days-old organoids of UT-SCC-42A and 42B with FLI-06 for 6 days. (F) Spheroid size of mature organoids over entire treatment period (0–6 days). (G) Effect of 2.5 μM FLI-06 on mRNA expression of Notch signaling genes in UT-SCC-42B cells after 72 hours of treatment, analyzed by qRT-PCR ($2^{-\Delta\Delta Ct}$). (H) The protein levels of NOTCH receptors (Notch1 - full length of NOTCH1 receptor; NICD1/3 - cleaved form of NOTCH1 and NOTCH3) and Notch downstream genes (HES1, HES5) in UT-SCC-42A and UT-SCC-42B cells after 48-h and 72-h exposure to FLI-06 assessed by Western blotting. Loading control: β-actin to standardize total amount of protein. (I) Impact of FLI-06 exposure on the intracellular expression and localization of NOTCH1 (blue), E-cadherin (green), and F-actin (red) in UT-SCC-42A cells.

calculated for UT-SCC-60A cells with a low Notch signature (Fig. 2G).

3.3. Combinatorial effects of FLI-06 and DTX treatment on HNSCC cell cycle and apoptosis

To elucidate the basis for the functional synergistic interaction of **FLI-06** and **DTX** in HNSCC cells, detailed analyses of the cell cycle progression and induction of apoptosis were performed. Based on previous experiments, the **FLI-06/DTX** sensitive SCC-9 line was selected as an experimental model. Firstly, we assessed distribution of cells in phases of cell cycle for the SSC-9 cell line after exposure to **FLI-06**, **DTX**, and combination of both compounds (Fig. 3A). The 48-hour exposure of 1, 2.5 and 5 μM **FLI-06** to cells indicated a dose-dependent accumulation of cells in the G_1 phase, with a concurrent decrease in the number of cells in S and G_2-M phases. Additionally, accumulation of cells in the pre-G1 phase (control 1.36 ± 0.2 % vs FLI-06 12.88 ± 0.6 %) was observed when SCC-9 cells were exposed to 5 μM of **FLI-06**. As expected for a taxane blocking tubulin turnover during mitosis, **DTX** resulted in accumulation of cells in the G_2-M phase, with a concurrent depletion in the number of cells in G_1 phase. Additionally, after **DTX** treatment, a dose-dependent accumulation of cells in pre-G_1 phase was observed. The combination of **FLI-06** and **DTX** resulted in major changes in all phases of the cell cycle for SCC-9 cells. Drug combination resulted in a dose-dependent accumulation of cells in the pre-G_1, and G_1, with a concurrent decrease in the number of cells in the S, and G_2-M phases. Interestingly, the lower concentrations of **FLI-06** and **DTX** combined (1 μM, and 1 nM, respectively) showed more similarity to the cell cycle changes resulted by **DTX** alone, while high concentrations of both drugs combined (5 μM and 5 nM, respectively) were strikingly similar to the **FLI-06** exposure, indicating that FLI-06 appears to dominate the drug-induced effects at higher concentrations.

Next, to reveal details concerning the molecular basis of the HNSCC cell cycle disturbances observed, we evaluated mRNA expression of cyclins and cyclin-dependent kinases, including Cyclin D1, A2, B1, and E1 (*CCND*1, *CCNA2*, *CCNB1*, *CCNE1*), and their inhibitors $p21^{Cip1/Waf1}$ and $p27^{Kip1}$ (*CDKN1A*, and *CDKN1B*), (Fig. 3B). Both **FLI-06** and **DTX** exposure led to a significant decrease in the expression of Cyclins D, A, and B mRNA. This effect persists after combination of both drugs. **FLI-06** (but not **DTX**) treatment also leads to increased $p21^{Cip1/Waf1}$ expression, and this effect was also observed when **FLI-06** was combined with **DTX**. Treatment with only **DTX** alone reduced the $p27^{Kip1}$ level. Interestingly, this effect was abolished by **FLI-06/DTX** co-treatment. Finally, opposing effects of **FLI-06** (increase) and **DTX** (decrease) treatment were observed for cyclin E1. The combination of both drugs resulted in the maintenance of cyclin E1 levels at the control level.

Next, we investigated potential pro-apoptotic properties of **FLI-06** and **DTX** alone and in combination. This was investigated by Annexin V and Propidium Iodide (PI) staining (Fig. 3C). Strong, dose-dependent accumulation of the apoptotic cells was observed for the SCC-9 cell line after exposure to both **FLI-06** and **DTX.** Compared to control cells, in which the level of early and late apoptosis was estimated at 4.6 ± 0.1 %, the level of apoptotic cells after treatment with 1, 2.5, and 5 μM FLI-06 was estimated at 5.7 ± 0.3 %, 12.5 ± 0.8 % and 20.1 ± 1.3 %, respectively. Apoptosis level for cells treated with 1, 2.5, and 5 nM **DTX** were estimated at 5.8 ± 0.3 %, 8.6 ± 0.6 % and 16.9 ± 0.5 %, respectively. The **FLI-06** and **DTX** combination resulted in a further increase in the levels of apoptotic cells to 16.6 ± 0.8 and 29 ± 1.2 %, for 2.5 μM FLI-06/2.5 nM DTX, and 5 μM FLI-06/ 5 nM DTX, respectively. Therefore, the combination of **FLI-06** and **DTX** showed a stronger pro-apoptotic effect in SCC-9 cells, compared to the effects of each compound alone.

To validate the ability of **FLI-06** and **DTX** to induce apoptosis in HNSCC cells, the levels of active caspase 3 was also assessed (Fig. 3D). The 48-hour exposure of **FLI-06** and **DTX** to SCC-9 cells resulted in a statistically significant increase in the number of cells with active-caspase 3. Similar to the Annexin V assay, this effect was again more pronounced with the combination of **FLI-06** and **DTX** compared to single drug treatments.

3.4. Molecular basis of FLI-06/DTX interaction

To elucidate the molecular mechanisms of the synergistic action of **FLI-06** and **DTX**, analyzes of the levels of expression and phosphorylation of key proteins related to the processes of proliferation, cell cycle and apoptosis were carried out using Phospho-Kinase array assays. Of the 39 proteins tested on the array (Fig. 4A, B Supplement, Fig. 1), the most significant changes were observed for c-Jun (S63 phosphorylation), P-38α (T180/Y182 phosphorylation) and GSK-3α/β (S21/S9 phosphorylation). **FLI-06** treatment resulted in a significant increase of $c\text{-}Jun^{S63}$ and MAP kinase $P\text{-}38\alpha^{T180/Y182}$ phosphorylation. An increase of $P\text{-}38\alpha^{T180/Y182}$ phosphorylation was observed for **DTX** exposure alone, but also when **DTX** was combined with **FLI-06**. Additionally, **DTX** treatment showed an increase of $GSK\text{-}3\alpha/\beta^{S21/S9}$ phosphorylation concurrent with a decrease of $c\text{-}Jun^{S63}$ phosphorylation.

Interestingly, **FLI-06** and **DTX** exposure resulted in opposite effects on c-Jun Serine 63 phosphorylation levels, which required further investigation. Therefore, the phosphorylation status of c-Jun under **FLI-06** and **DTX** was assessed in SCC-9 and UT-SCC-44 cell lines (Fig. 4C). For the SSC-9 line, **FLI-06**-dependent increase, and **DTX**-dependent decrease in $c\text{-}Jun^{S63}$ phosphorylation was confirmed. Additionally, **FLI-06** caused increased $c\text{-}Jun^{S243}$ phosphorylation, however combination of **FLI-06** with **DTX** decreased the level of $c\text{-}Jun^{S243}$. For UT-SCC-44 cells, **FLI-06**, and **DTX** dependent changes of $c\text{-}Jun^{S63}$ and $c\text{-}Jun^{S243}$ phosphorylation was not observed. Interestingly, combination of both drugs resulted significant decrease of $c\text{-}Jun^{S63}$ and $c\text{-}Jun^{S243}$ phosphorylation. Finally, for SCC-9 and UT-SCC-44 cells, the decrease in phosphorylation of $c\text{-}Jun^{S243}$ was dependent on the increase of **DTX** concentration.

Additionally, in the SCC-9 line, an increased expression of the pro-apoptotic BAX protein was confirmed by **FLI-06**, **DTX** and both drugs in combination (Fig. 4C). Surprisingly, BAX levels showed an inverse relationship with **DTX** concentration. The lowest **DTX** concentration (0.5 nM) in combination with 1 μM **FLI-06** induced the highest increase of BAX expression. None of the tested drugs or their combinations influenced the expression of BAX in the UT-SCC-44 cells.

3.5. FLI-06 and DTX interaction in the Danio rerio fish model

The zebrafish model (*Danio rerio*) was used to investigate the anti-tumour potential of **FLI-06**, and **FLI-06/DTX** combinations in *in vivo*

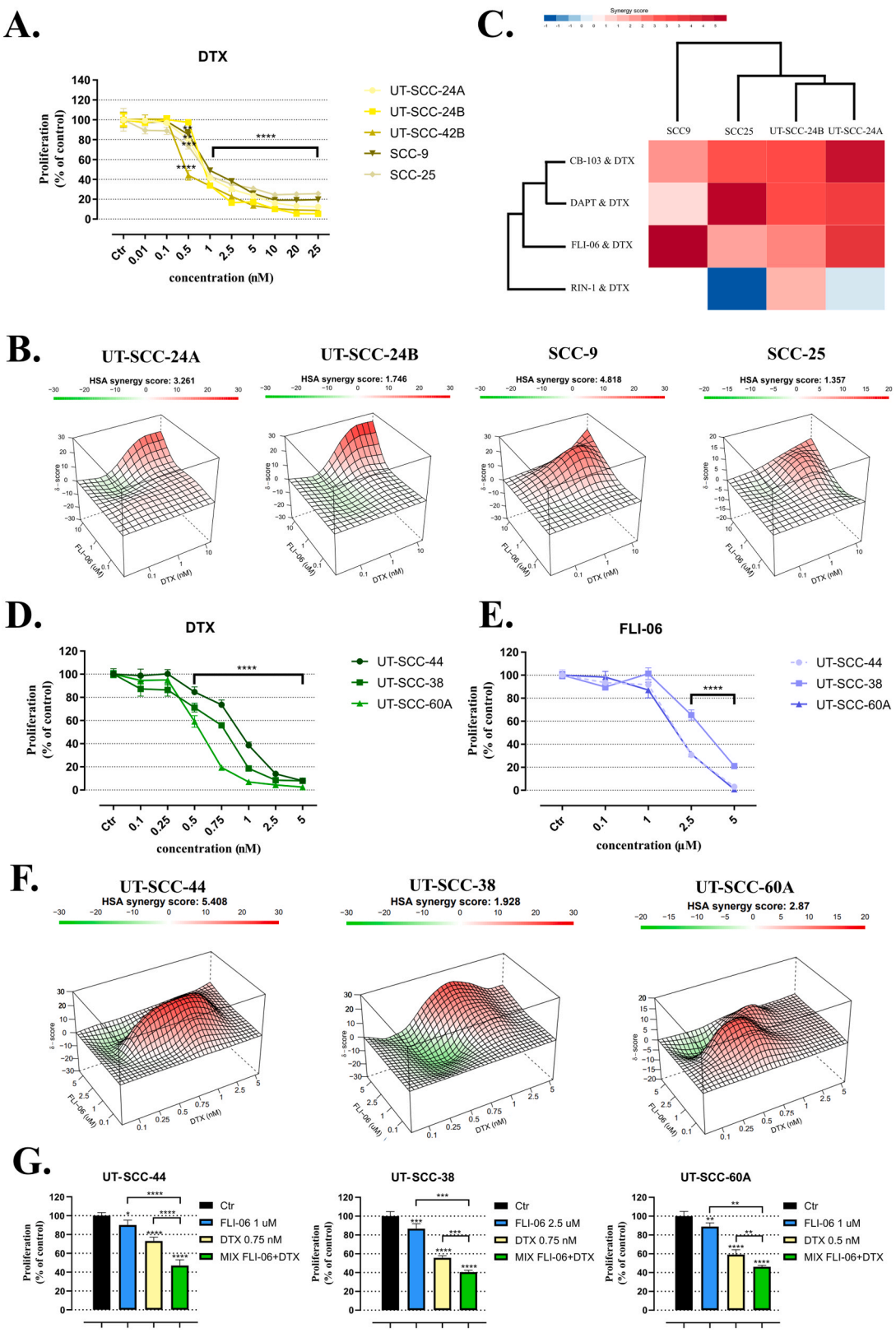

Fig. 2. Analysis of FLI-06 and DTX drug combination in HNSCC. (A) Cell proliferation (% of control) after DTX treatment at the endpoint of experiments (96 h) assessed by MTT assay. (B) HSA synergy score and 3D synergy maps for a FLI-06 (0.1–10 μM) and DTX (0.1–10 nM) combinations in HNSCC cells. The red area indicates synergistic, and green antagonistic interaction between the tested drugs. (C) A heatmap showing the synergy patterns (red synergistic; blue antagonistic) for the combination of Notch signaling inhibitors (CB-103, DAPT, FLI-06), activator (RIN-1), with DTX in HNSCC cell lines. (D) Cell proliferation (% of control) after DTX and (E) FLI-06 treatment at the endpoint of experiments (96 h), as assessed by MTT assay for high (UT-SCC-44), medium (UT-SCC-38), and low (UT-SCC-60A) Notch signaling signature HNSCC cell lines. (F) HSA synergy score and 3D synergy maps for a FLI-06 (0.1–5 μM) and DTX (0.1–5 nM) combinations in HNSCC cells. (G) Cell proliferation (% of control) for FLI-06, DTX and combination of both drugs in MSA (the most synergistic area).

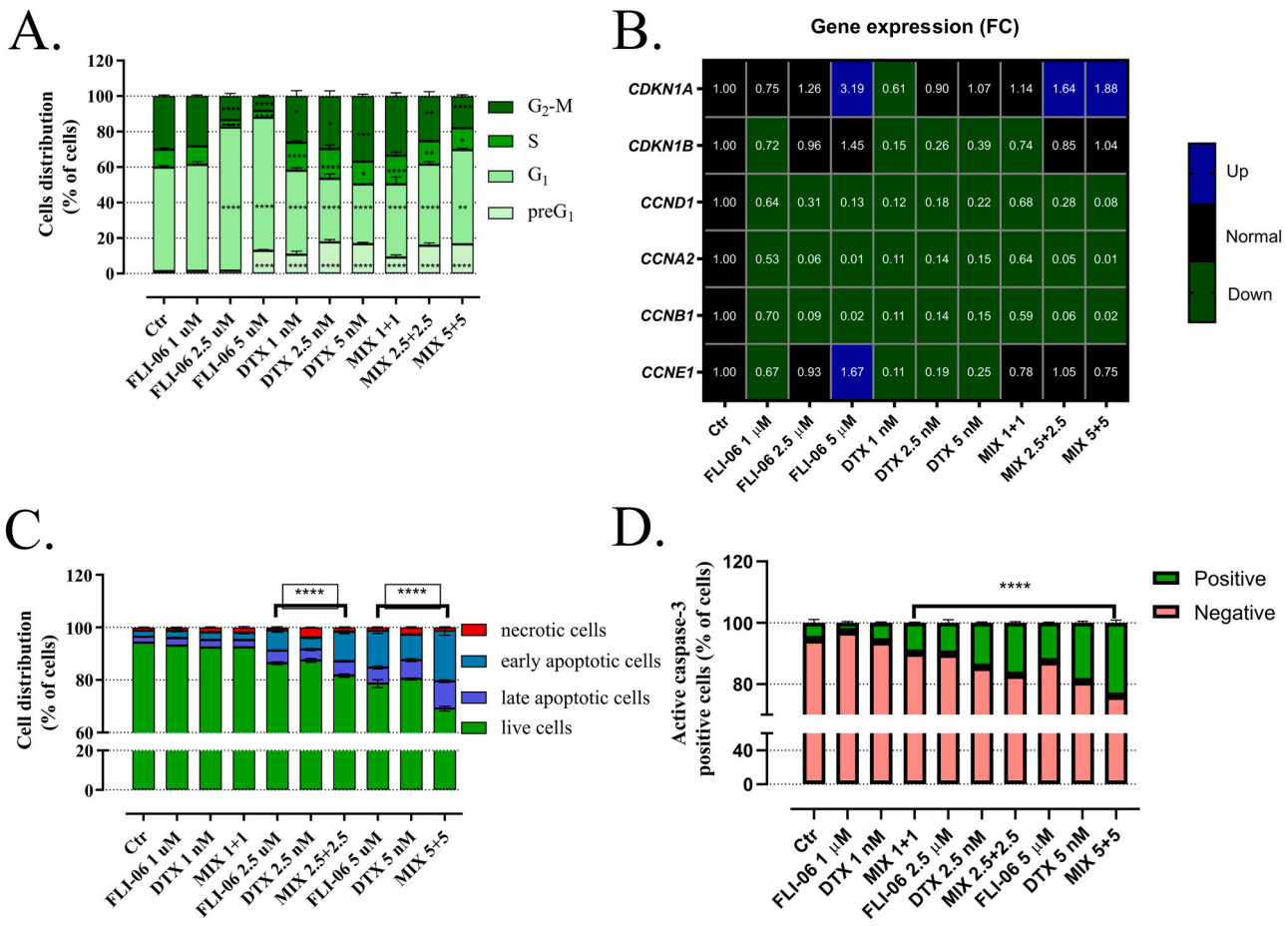

Fig. 3. The effect of FLI-06 and DTX on HNSCC cells cell cycle and apoptosis. (A) SCC-9 cells were treated with 1, 2.5 and 5 μM of FLI-06, 1, 2.5 and 5 nM of DTX, and combination of both drugs for 48 h. The percentage of cells in each phase of the cell cycle marked by the propidium iodide (PI) staining method. (B) The effects of the drugs on expression of cell cycle-related genes, as analysed by qRT-PCR ($2^{-\Delta\Delta Ct}$). (C) The percentage of necrotic, early, and late apoptotic cells versus viable cells was assessed by Annexin V/Propidium Iodide (PI) staining assay. (D) Activation of caspase-3 in cells assessed by phycoerythrin (PE)-conjugated antibody staining.

conditions. Drugs in E3 buffer was added to the 2-dpf fish larvae immediately after SCC-9 cells injection. Next, the fish were monitored for 3 days every 24 h. Compared to the control (untreated, cancer cells-injected fish), a decrease in HNSCC tumour size was observed, in both **FLI-06**, **DTX** and combination of **FLI-06/DTX** treated fish (Fig. 5A, B).

Additionally, to investigate the mRNA expression levels and reveal changes of HNSCC cells implanted into fish, a series of qPCR experiments were performed. After 72 h drug treatment (by adding the compounds to the water), a decrease in the expression of tumour-derived human *GAPDH* RNA was observed (Fig. 5C), with a concomitant increase in the expression of human *CDKN1A* (Fig. 5D), and *BAX* (Fig. 5E). Again, these effects were more pronounced with the combination of **FLI-06** and **DTX** compared to treatment by each compound alone. Only by combining 1 μM FLI and 1 nM DTX, a significant and reproducible decrease in *BAX* expression was observed compared to single drugs.

4. Discussion

In this study, we identify **FLI-06** as a potent inhibitor of the Notch signaling pathway in head and neck cancer cells, and show its usefulness in combinatorial drug therapy, especially in combination with taxanes. The anti-tumour effects of **FLI-06** is linked to its interference with the transport of NOTCH receptors from the endoplasmic reticulum through the Golgi apparatus, and blocking of the transport of pre-mature Notch receptors [11] to the cell membrane. Based on our presented results, we speculate that decreased amounts of mature NOTCH receptors may attenuate Notch signaling pathway activity, which may consequently lead to the inhibition of proliferation and growth of HNSCC cell lines. It may also interfere with maturation and formation of organoids generated from HNSCC cell lines. This interpretation would be consistent with results presented by other groups. The general effect of using **FLI-06** in esophageal squamous cell carcinoma (ESCC) [12] and tongue squamous cell carcinoma (TSCC) [13] cells was a reduction/block of cell proliferation, induction of apoptosis, and arrest of the cells in the G_1 phase of the cell cycle. These observations are consistent with our results in HNSCC cell lines tested in both 2D and 3D conditions.

In the present study, we demonstrated a beneficial effect of Notch signaling inhibition on the sensitivity of HNSCC cells to taxane treatment. Our data show that relatively low, non-toxic **FLI-06** (1–10 μM) and DTX concentrations (1–10 nM) result in measurable synergistic effects, as indicated by a significant reduction of HNSCC cell proliferation. Combining not only **FLI-06** but also other Notch inhibitors such as **CB-103**, and **DAPT** with **DTX** demonstrated their additive model of action. Interestingly, this effect declined (or even became antagonistic) when the Notch signaling activator, **RIN-1**, was used. This demonstrates that Notch signaling activities are critical for taxane sensitivity. Additionally, we have shown that HNSCC cell lines characterized by strong and possibly hyperactivated Notch signaling, such as UT-SCC-44 and UT-SCC-38, achieve a better response to **DTX** treatment, compared to low-Notch cells, such as UT-SCC-60A, when treatment is combined with **FLI-06**. This results clearly links Notch signaling to taxane resistance. In contrast, we can only assume that active Notch signaling status may be critical for **FLI-06** to unfold its full biochemical activities, although we have not seen a clear correlation in our cell lines. Nevertheless, we

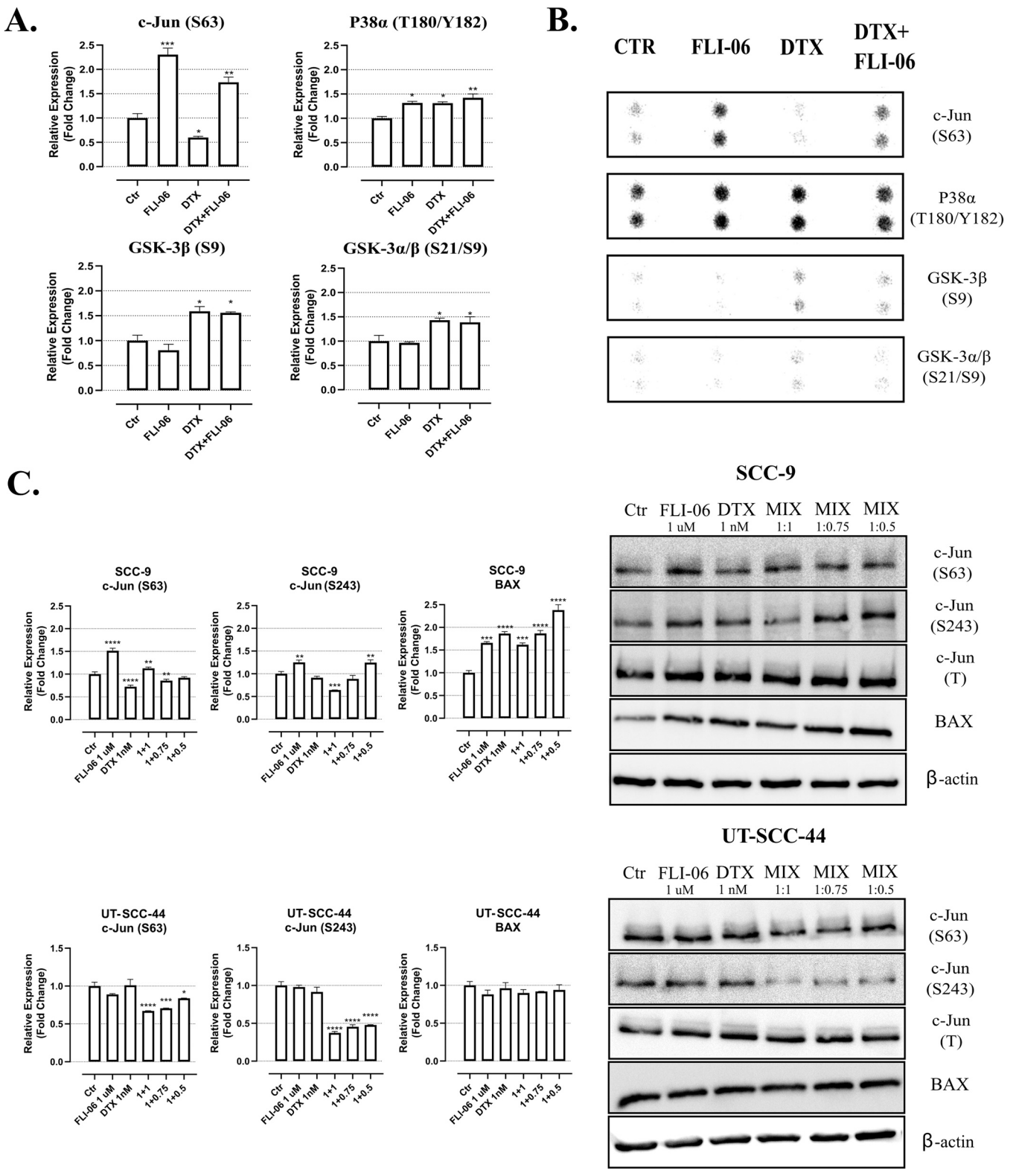

Fig. 4. Immunoblotting of P-c-Jun and BAX in HNSCC cells after FLI-06, DTX and combination treatment. SCC-9 cells were treated with 1 μM FLI-06, 1 nM DTX and a combination of both drugs (1 μM FLI-06, and 1 nM DTX). Protein phosphorylation was determined after 48 h cells incubation with drugs by phosphorylation arrays assay kit. Densitometric analysis (A) and representative dot-blots (B) of c-Jun^{S63}, P-38α$^{T180/Y182}$, GSK-3β^{S9}, and GSK-3α/β$^{S21/S9}$. (C) C-Jun phosphorylation status, and BAX protein level in SCC-9 and UT-SCC-44 cells after 48-h exposure to 1 μM FLI-06, 1 nM DTX and combination of both drugs (MIX; 1 μM FLI-06 and 1;0.75.0.5 nM DTX, respectively) assessed by Western blotting. β-actin and c-Jun (T: Total); internal control of amount of protein. Representative blots and densitometric analysis are shown.

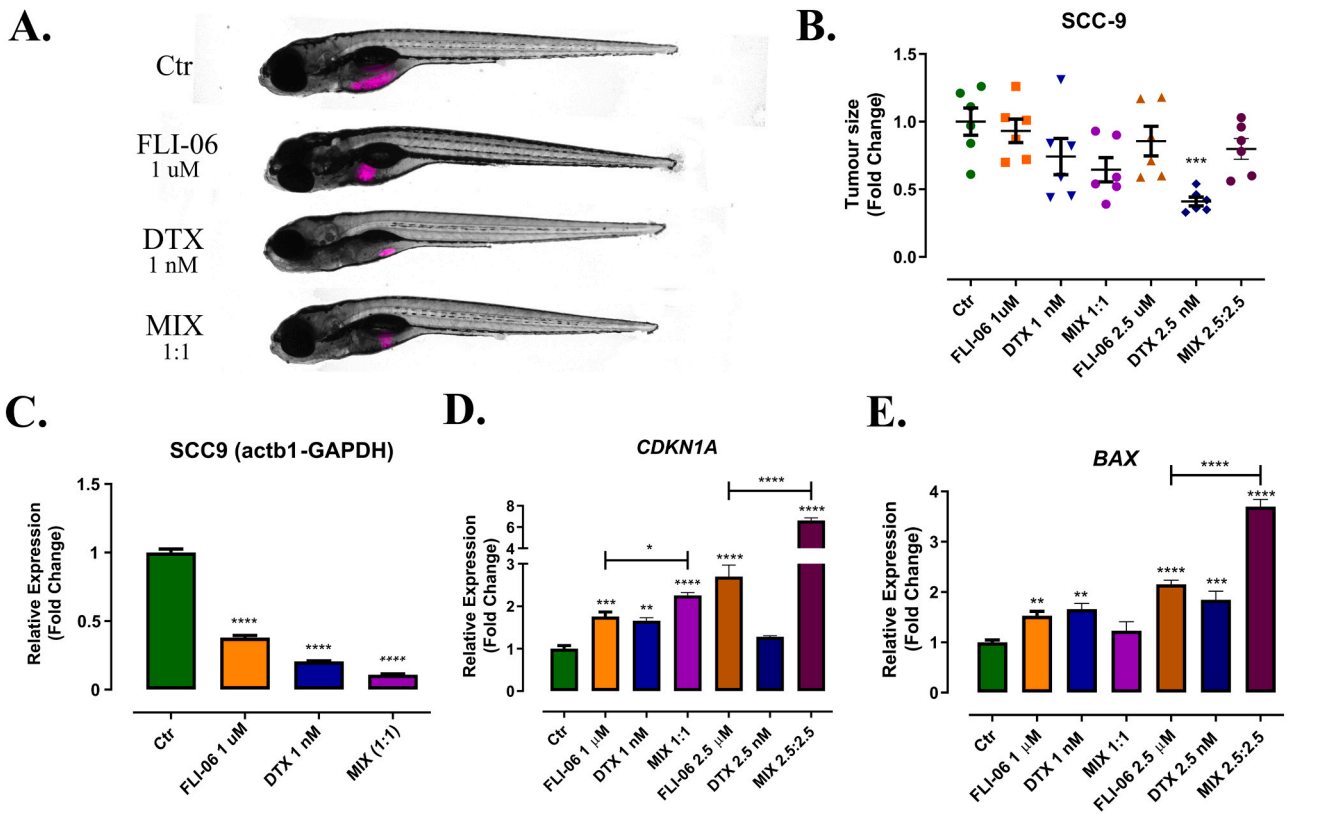

Fig. 5. The effects of FLI-06, DTX and combination treatments of HNSCC cells implanted into the *Danio rerio* fish model. (A) The effects of 72 h of FLI-06, DTX and combination of both drugs treatment on SCC-9 cells xenografts. Representative pictures taken 5 days post fertilization (dpf). (B) Vybrant DiD-stained SCC-9 cells were transplanted into fish larvae treated with 1–2.5 μM FLI-06, 1–2.5 nM DTX and combination of both compounds. Tumour size (total xenografts area; n = 6 fish) 5 dpf, based on quantification of Vybrant DiD fluorescence, shown as fold change of control. (C, D, E) The effects of drug exposure on mRNA expression of human *GAPDH* and zebrafish β-actin as a housekeeping gene (C), *CDKN1A* (D), and *BAX* (E) of SCC-9 cells in 5 dpf fish assessed by the qPCR method.

observe that cell lines that lack NOTCH expression, or have very low activity, are poorly responsive to FLI-06.

Until now, several examples linking the Notch signaling and taxane resistance have been presented in the literature. It was shown that treatment with taxanes may lead to an enrichment of cancer stem cell (CSC) populations, accompanied by NOTCH1 overexpression in these cells. Subsequently, down-regulation of NOTCH1 has resulted in an increase in the sensitivity of CSCs to taxanes [18]. Similarly, NOTCH1 and JAG1 inhibition via miR-34a increased chemosensitivity of prostate cancer to paclitaxel [20]. Mechanistically, it has been shown that excessive Notch signaling is associated with increased expression of multi-drug resistance protein (MDR) via Notch-1/AP-1/MDR-1 axis. Consequently, inhibition of NOTCH1 sensitizes lung adenocarcinoma to **DTX** [21]. The effects in HNSCC will likely be more differentiated as we expect to observe partial compensation of NOTCH1 loss-of-function mutations by other Notch receptors, and the overall activity of the pathway has to be considered.

The cell cycle data presented here reveal that **FLI-06** and **DTX** act in two different phases of the cell cycle, with **FLI-06** arresting cells in G_1-S phase transition, and **DTX** acting in mitosis, resulting in a block of cells in G_2-M phase. The use of the combination of both drugs should therefore target different mechanisms of actions, which we assumed could result in synergistic or at least strongly additive effects compared to single drug treatments. Indeed, the combinatorial treatment results in a very significant and additive to synergistic disruption of the cell cycle progression that involved at least two phases, which may reflect the impact from both tested drugs. Additionally, the combination of **FLI-06** and **DTX** seems to markedly be more effective in inducing apoptosis in the tested HNSCC cells than either compound alone. Thus, mutual promotion of apoptosis appears to be one of the main mechanisms of interaction between Notch inhibition and **DTX** [19], which was also confirmed in our research. However, according to our observations, the concentrations of **FLI-06** and **DTX** used in the combination treatment are crucial for the effective enhancement of apoptosis. When examining the expression level of the pro-apoptotic BAX protein and its mRNA, it was observed that combining only lower-level concentration of 1 μM **FLI-06** with 1 nM **DTX** works less effectively than either drug alone, i.e., lacking additive potentiation. However, the level of BAX expression was increased over the levels in individual treatments when **DTX** concentration was gradually reduced (as measured by the protein level) or the concentration of both substances was increased (mRNA levels measured *in vivo* in the zebrafish model). These results indicate the important role of appropriate drug dosing and drug bioavailability to predict adequate therapeutic response.

Currently, data regarding the crosstalk of Notch signaling with c-Jun/AP-1 regulators of gene expression are still incomplete. It is established that c-Jun/AP-1 is critical for regulation of proliferation versus differentiation in epithelial cells, including squamous epithelial cells (keratinocytes). This represents a natural overlap with the functions of the Notch pathway deciding cell fate and tissue-specific maturation in squamous epithelial cells. Thus, dysregulation of c-Jun would be in line with the role of Notch receptors as tumor suppressors in early-stage cancer initiation by blocking terminal differentiation of squamous cells in the skin, oral mucosa, cervix, lung, and esophagus [35,36]. This role may be reverted in advanced, recurrent, and metastatic HNSCC in which Notch signaling may act predominantly in an oncogenic fashion, at least in a subset of tumors and cell lines.

It is known that the presence of an active NICD represses AP-1 activity [37]. Additionally, NICD inhibits the activation of c-Jun N-terminal kinase (JNK), responsible for c-Jun activation [38] activity and

expression. In our studies, we demonstrated two key effects for **FLI-06** and **DTX** interaction for c-Jun activity. Firstly, we showed that **FLI-06** induced the phosphorylation of c-Jun on serine 63 (C-Jun^{S63}). Second, we showed that **DTX** increases the suppressive phosphorylation of GSK-3β on serine 9 (GSK-3β^{S9}), which keeps GSK-3β in an inactive state. Additionally, we show that the combinatorial use of **FLI-06** and **DTX** leads to a decrease in C-Jun^{S243} phosphorylation. Therefore, we suggest that **DTX**, by blocking the activity of GSK-3β (GSK-3β^{S9}), leads to an increased stability of c-Jun (lack of C-Jun^{S243}), a process which is additionally activated via blocking Notch by **FLI-06** (enhancing c-Jun^{S63}). Consequently, the combination of **FLI-06** and **DTX** may promote c-Jun/AP-1 dependent signaling and activation of target gene expression (Fig. 6). Our data suggest that blocking Notch signaling may result in increased (hyper-)activity of c-Jun, which consequently promotes the activity of AP-1 – which in turns may induce terminal squamous differentiation, derange cell cycle progression, and/or induce apoptosis.

Nevertheless, several aspects should be kept in mind when combining the anticancer activity of **FLI-06** with the inhibition of Notch signaling. It is possible that, as a consequence of **FLI-06** being an endoplasmic reticulum traffic inhibitor, not only NOTCH but also a number of other transmembrane receptors and proteins may not be properly translocated to the cell surface, with consequences to their signaling activity. This can lead to significant changes in cell metabolism, at least partly unrelated to Notch signaling. It is debated but remains currently unclear if inhibition and/or changes in the half life, trafficking and intracellular activity of Notch signaling components plays a role in drug resistance of HNSCC cells and tissues. Hyperactivation of Notch signaling may be indeed beneficial for later stage tumour progression, and is associated with chemoresistance of advanced HNSCC lesions; potentially similar to the effects observed in Triple-Negative Breast Cancer [39]. Thus, **FLI-06**-related inhibition of Notch signaling may find application in such cases. On the other hand, it was shown that loss-of-function mutations of core proteins of Notch signaling pathway, primarily the NOTCH receptors themselves, are mainly beneficial for the initiation of HNSCC lesions in some patients and may act as a gatekeeper for acquisition of additional mutations that eventually lead to early-stage, tumorigenic transformation. Later stage reversal of this situation, especially in advanced, recurrent and metastatic HNSCC, might be based on a) the possibility of functional compensation between different NOTCH receptors, b) extending the functional half-life of the NICD in tumor cells, and c) the re-expression of epigenetically silenced expression patterns that can also occur at later stages. The impact of epigenetics changes requires special attention because **FLI-06** has also been shown to inhibit the expression of LSD1 (histone lysine-specific demethylase 1, a transcriptional activator that is associated with promoting the development of HNSCC [12]) and may cooperate with Notch signaling. In our studies, we have not analyzed the genetic or epigenetic differences between HNSCC cells but there are no very significant differences in the effectiveness of the tested drugs in 2D and 3D conditions for **DTX**, which can be observed using 2D monolayer cultures for our experiment with **FLI-06**.

5. Conclusion

Our studies demonstrate a positive effect of combining Notch signaling inhibitors, such as **FLI-06** with taxanes to inhibit HNSCC cell growth. This effect may be particularly beneficial in cells with intense Notch signaling. The mechanism of interaction between **FLI-06** and **DTX** is related to cell cycle aberration and induction of apoptosis, which is accompanied by a change in the c-Jun phosphorylation status. Our data shows beneficial outcomes of combined treatment of Notch inhibitors and taxanes compounds for HNSCC therapy.

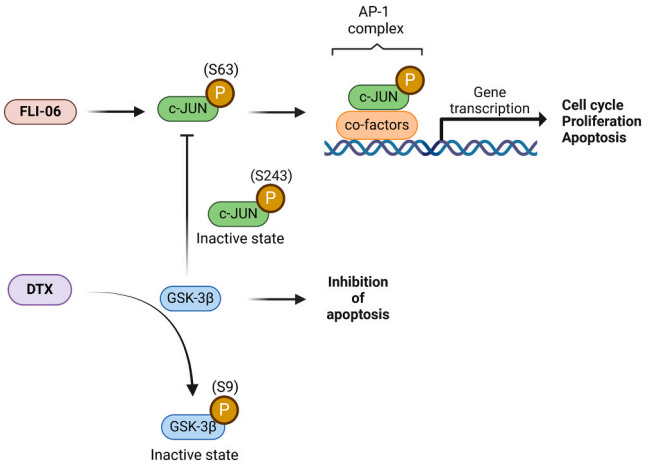

Fig. 6. FLI-06 induces phosphorylation of c-Jun on serine 63 (C-Jun^{S63}) leads to an increase in the stability and activity of c-Jun as part of the AP-1 complex. DTX increases the suppressive phosphorylation of GSK-3β on serine 9 (GSK-3β^{S9}) which keeps GSK-3β in inactive state, preventing GSK-3β-depending suppressive C-Jun^{S243} phosphorylation.

Ethics approval and consent to participate

The study was conducted according to the guidelines, and approved by the Ethics Committees and Institutional Review Board of the Medical University of Lublin. The study complied with the relevant ethical regulations for animal research.

Consent for publication

All authors agree to publication.

Funding

This research was funded by the Polish National Science Centre (NCN): UMO-2020/37/B/NZ4/03920, DEC-2021/41/B/NZ7/03786, and DEC-2021/41/N/NZ5/01938 and Polish National Agency for Academic Exchange (NAWA): PPI/APM/2019/1/00089/U/00001, Internal project "Grant innowacyjny G7" of Medical University of Lublin, and Jane & Aatos Erkko Foundation, project "Matrix Matters".

CRediT authorship contribution statement

Mervi Toriseva: Supervision, Resources, Project administration, Methodology, Investigation, Data curation. **Matthias Nees:** Writing – review & editing, Writing – original draft, Supervision, Resources, Project administration, Funding acquisition. **Shaoxia Wang:** Methodology, Investigation, Data curation. **Alicja Przybyszewska-Podstawka:** Methodology, Investigation, Data curation. **Arkadiusz Czerwonka:** Writing – review & editing, Writing – original draft, Visualization, Validation, Resources, Project administration, Methodology, Investigation, Funding acquisition, Formal analysis, Data curation, Conceptualization. **Joanna Kałafut:** Writing – review & editing, Visualization, Validation, Resources, Methodology, Investigation, Funding acquisition, Data curation.

Declaration of Competing Interest

The authors declare that they have no known competing financial interests or personal relationships that could have appeared to influence the work reported in this paper.

Data Availability

Data will be made available on request.

Acknowledgements

The authors would like to thank to colleagues from FICAN West Cancer Centre Laboratory of University of Turku for warmly welcome, Sima spring mead and enjoyable working atmosphere in Finland.

Appendix A. Supporting information

Supplementary data associated with this article can be found in the online version at doi:10.1016/j.biopha.2024.116822.

References

[1] B. Zhou, W. Lin, Y. Long, Y. Yang, H. Zhang, K. Wu, Q. Chu, Notch signaling pathway: architecture, disease, and therapeutics, 2022 71, Signal Transduct. Target. Ther. 7 (2022) 1–33, https://doi.org/10.1038/s41392-022-00934-y.

[2] J. Kałafut, A. Czerwonka, A. Anameriç, A. Przybyszewska-Podstawka, J. O. Misiorek, A. Rivero-Müller, M. Nees, Shooting at moving and hidden targets-tumour cell plasticity and the notch signalling pathway in head and neck squamous cell carcinomas, Cancers 13 (2021), https://doi.org/10.3390/CANCERS13246219.

[3] P.A. Shah, C. Huang, Q. Li, S.A. Kazi, L.A. Byers, J. Wang, F.M. Johnson, M. J. Frederick, NOTCH1 signaling in head and neck squamous cell carcinoma, Cells 9 (2020), https://doi.org/10.3390/cells9122677.

[4] L. Gragnani, S. Lorini, S. Marri, A.L. Zignego, Role of notch receptors in hematologic malignancies, Cells 10 (2021), https://doi.org/10.3390/cells10010016.

[5] M. xi Xiu, Y. meng Liu, B. hai Kuang, The oncogenic role of Jagged1/Notch signaling in cancer, Biomed. Pharmacother. 129 (2020), https://doi.org/10.1016/j.biopha.2020.110416.

[6] A.N. Weaver, M.Benjamin Burch, T.S. Cooper, D.L.D. Manna, S. Wei, A.I. Ojesina, E.L. Rosenthal, E.S. Yang, Notch signaling activation is associated with patient mortality and increased FGF1-mediated invasion in squamous cell carcinoma of the oral cavity, Mol. Cancer Res. 14 (2016), https://doi.org/10.1158/1541-7786.MCR-16-0114.

[7] S.S. Islam, K. Qassem, S. Islam, R.R. Parag, M.Z. Rahman, W.A. Farhat, H. Yeger, A. Aboussekhra, B. Karakas, A. Shadat, M. Noman, Genetic alterations of Keap1 confers chemotherapeutic resistance through functional activation of Nrf2 and Notch pathway in head and neck squamous cell carcinoma, 2022 138, Cell Death Dis. 13 (2022) 1–13, https://doi.org/10.1038/s41419-022-05126-8.

[8] S. Pongjantarasatian, N. Nowwarote, V. Rotchanakitamnuai, W. Srirodjanakul, R. Saehun, K. Janebodin, J. Manokawinchoke, B.P.J. Fournier, T. Osathanon, A γ-secretase inhibitor attenuates cell cycle progression and invasion in human oral squamous cell carcinoma: an in vitro study, Int. J. Mol. Sci. 23 (2022), https://doi.org/10.3390/ijms23168869.

[9] Y. Zou, F. Fang, Y.J. Ding, M.Y. Dai, X. Yi, C. Chen, Z.Z. Tao, S.M. Chen, Notch 2 signaling contributes to cell growth, anti-apoptosis and metastasis in laryngeal squamous cell carcinoma, Mol. Med. Rep. 14 (2016), https://doi.org/10.3892/mmr.2016.5688.

[10] A. Czerwonka, J. Kałafut, S. Wang, A. Anameric, A. Przybyszewska-Podstawka, J. Mattsson, M. Karbasian, D. Le Manach, M. Toriseva, M. Nees, Evaluation of the anticancer activity of RIN-1, a Notch signaling modulator, in head and neck squamous cell carcinoma, Sci. Rep. 13 (2023), https://doi.org/10.1038/s41598-023-39472-0.

[11] A. Krämer, T. Mentrup, B. Kleizen, E. Rivera-Milla, D. Reichenbach, C. Enzensperger, R. Nohl, E. Täuscher, H. Görls, A. Ploubidou, C. Englert, O. Werz, H.D. Arndt, C. Kaether, Small molecules intercept Notch signaling and the early secretory pathway, 2013 911, Nat. Chem. Biol. 9 (2013) 731–738, https://doi.org/10.1038/nchembio.1356.

[12] Z. Lu, Y. Ren, M. Zhang, T. Fan, Y. Wang, Q. Zhao, H.M. Liu, W. Zhao, G. Hou, FLI-06 suppresses proliferation, induces apoptosis and cell cycle arrest by targeting LSD1 and Notch pathway in esophageal squamous cell carcinoma cells, Biomed. Pharmacother. 107 (2018) 1370–1376, https://doi.org/10.1016/J.BIOPHA.2018.08.140.

[13] R.H. Gan, L.S. Lin, J. Xie, L. Huang, L.C. Ding, B.H. Su, X.E. Peng, D.L. Zheng, Y. G. Lu, FLI-06 intercepts notch signaling and suppresses the proliferation and self-renewal of tongue cancer cells, Oncol. Targets Ther. 12 (2019) 7663–7674, https://doi.org/10.2147/OTT.S221231.

[14] M. Zhang, Y. Han, Y. Zheng, Y. Zhang, X. Zhao, Z. Gao, X. Liu, ZEB1-activated LINC01123 accelerates the malignancy in lung adenocarcinoma through NOTCH signaling pathway, Cell Death Dis. 11 (2020) 1–14, https://doi.org/10.1038/s41419-020-03166-6.

[15] S.M. Maloney, C.A. Hoover, L.V. Morejon-Lasso, J.R. Prosperi, Mechanisms of taxane resistance, Cancers 12 (2020), https://doi.org/10.3390/cancers12113323.

[16] L. Mosca, A. Ilari, F. Fazi, Y.G. Assaraf, G. Colotti, Taxanes in cancer treatment: activity, chemoresistance and its overcoming, Drug Resist. Updat. 54 (2021), https://doi.org/10.1016/j.drup.2020.100742.

[17] S. Zang, F. Chen, J. Dai, D. Guo, W. Tse, X. Qu, D. Ma, C. Ji, RNAi-mediated knockdown of Notch-1 leads to cell growth inhibition and enhanced chemosensitivity in human breast cancer, Oncol. Rep. 23 (2010), https://doi.org/10.3892/or-00000712.

[18] J. Mao, B. Song, Y. Shi, B. Wang, S. Fan, X. Yu, J. Tang, L. Li, ShRNA targeting Notch1 sensitizes breast cancer stem cell to paclitaxel, Int. J. Biochem. Cell Biol. 45 (2013), https://doi.org/10.1016/j.biocel.2013.02.022.

[19] Q.F. Ye, Y.C. Zhang, X.Q. Peng, Z. Long, Y.Z. Ming, L.Y. He, Silencing Notch-1 induces apoptosis and increases the chemosensitivity of prostate cancer cells to docetaxel through Bcl-2 and Bax, Oncol. Lett. 3 (2012), https://doi.org/10.3892/ol.2012.572.

[20] X. Liu, X. Luo, Y. Wu, D. Xia, W. Chen, Z. Fang, J. Deng, Y. Hao, X. Yang, T. Zhang, L. Zhou, Y. Wu, Q. Wang, J. Xu, X. Hu, L. Li, MicroRNA-34a attenuates paclitaxel resistance in prostate cancer cells via direct suppression of JAG1/Notch1 axis, Cell. Physiol. Biochem. 50 (2018), https://doi.org/10.1159/000494004.

[21] J. Huang, Y. Chen, J. Li, K. Zhang, J. Chen, D. Chen, B. Feng, H. Song, J. Feng, R. Wang, L. Chen, Notch-1 confers chemoresistance in lung adenocarcinoma to taxanes through AP-1/microRNA-451 Mediated Regulation of MDR-1, Mol. Ther. Nucleic Acids 5 (2016), https://doi.org/10.1038/mtna.2016.82.

[22] Z. Zhang, Z. Zhou, M. Zhang, N. Gross, L. Gong, S. Zhang, D. Lei, Q. Zeng, X. Luo, G. Li, X. Li, High Notch1 expression affects chemosensitivity of head and neck squamous cell carcinoma to paclitaxel and cisplatin treatment, Biomed. Pharmacother. 118 (2019) 109306, https://doi.org/10.1016/J.BIOPHA.2019.109306.

[23] Z.L. Zhao, L. Zhang, C.F. Huang, S.R. Ma, L.L. Bu, J.F. Liu, G.T. Yu, B. Liu, J. S. Gutkind, A.B. Kulkarni, W.F. Zhang, Z.J. Sun, NOTCH1 inhibition enhances the efficacy of conventional chemotherapeutic agents by targeting head neck cancer stem cell, Sci. Rep. 6 (2016), https://doi.org/10.1038/srep24704.

[24] A.G. Papavassiliou, A.M. Musti, The multifaceted output of c-Jun biological activity: focus at the junction of CD8 T cell activation and exhaustion, Cells 9 (2020), https://doi.org/10.3390/cells9112470.

[25] R.L. Eckert, G. Adhikary, C.A. Young, R. Jans, J.F. Crish, W. Xu, E.A. Rorke, AP1 transcription factors in epidermal differentiation and skin cancer, J. Ski. Cancer 2013 (2013), https://doi.org/10.1155/2013/537028.

[26] J. Whitfield, S.J. Neame, L. Paquet, O. Bernard, J. Ham, Dominant-negative c-Jun promotes neuronal survival by reducing BIM expression and inhibiting mitochondrial cytochrome c release, Neuron 29 (2001), https://doi.org/10.1016/S0896-6273(01)00239-2.

[27] D. Zhang, Q. Zhou, D. Huang, L. He, H. Zhang, B. Hu, H. Peng, D. Ren, ROS/JNK/c-Jun axis is involved in oridonin-induced caspase-dependent apoptosis in human colorectal cancer cells, Biochem. Biophys. Res. Commun. 513 (2019), https://doi.org/10.1016/j.bbrc.2019.04.011.

[28] Y.Y. Cho, F. Tang, K. Yao, C. Lu, F. Zhu, D. Zheng, A. Pugliese, A.M. Bode, Z. Dong, Cyclin-dependent kinase-3-mediated c-Jun phosphorylation at Ser63 and Ser73 enhances cell transformation, Cancer Res. 69 (2009), https://doi.org/10.1158/0008-5472.CAN-08-3125.

[29] W.J. Boyle, T. Smeal, L.H.K. Defize, P. Angel, J.R. Woodgett, M. Karin, T. Hunter, Activation of protein kinase C decreases phosphorylation of c-Jun at sites that negatively regulate its DNA-binding activity, Cell 64 (1991), https://doi.org/10.1016/0092-8674(91)90241-P.

[30] V. Härmä, J. Virtanen, R. Mäkelä, A. Happonen, J.P. Mpindi, M. Knuuttila, P. Kohonen, J. Lötjönen, O. Kallioniemi, M. Nees, A comprehensive panel of three-dimensional models for studies of prostate cancer growth, invasion and drug responses, PLoS One 5 (2010), https://doi.org/10.1371/journal.pone.0010431.

[31] A. Ianevski, A.K. Giri, T. Aittokallio, SynergyFinder 3.0: an interactive analysis and consensus interpretation of multi-drug synergies across multiple samples, Nucleic Acids Res. 50 (2022), https://doi.org/10.1093/nar/gkac382.

[32] Z. Ali, M. Vildevall, G.V. Rodriguez, D. Tandiono, I. Vamvakaris, G. Evangelou, G. Lolas, K.N. Syrigos, A. Villanueva, M. Wick, S. Omar, A. Erkstam, J. Schueler, A. Fahlgren, L.D. Jensen, Zebrafish patient-derived xenograft models predict lymph node involvement and treatment outcome in non-small cell lung cancer, J. Exp. Clin. Cancer Res. 41 (2022) 1–18, https://doi.org/10.1186/S13046-022-02280-X/FIGURES/6.

[33] T. Lepikhova, P.R. Karhemo, R. Louhimo, B. Yadav, A. Murumagi, E. Kulesskiy, M. Kivento, H. Sihto, R. Grenman, S.M. Syrjanen, O. Kallioniemi, T. Aittokallio, K. Wennerberg, H. Joensuu, O. Monni, Drug-sensitivity screening and genomic characterization of 45 HPV-negative head and neck carcinoma cell lines for novel biomarkers of drug efficacy, Mol. Cancer Ther. 17 (2018) 2060–2071, https://doi.org/10.1158/1535-7163.MCT-17-0733.

[34] B.C. Nguyen, K. Lefort, A. Mandinova, D. Antonini, V. Devgan, G. Della Gatta, M. I. Koster, Z. Zhang, J. Wang, A.T. Di Vignano, J. Kitajewski, G. Chiorino, D.R. Roop, C. Missero, G.P. Dotto, Cross-regulation between Notch and p63 in keratinocyte commitment to differentiation, Genes Dev. 20 (2006), https://doi.org/10.1101/gad.1406006.

[35] J.Y. Zhang, M.A. Selim, The role of the c-Jun N-terminal Kinase signaling pathway in skin cancer, Am. J. Cancer Res. 2 (2012).

[36] J.Y. Jin, H. Ke, R.P. Hall, J.Y. Zhang, C-Jun promotes whereas JunB inhibits epidermal neoplasia, J. Invest. Dermatol. 131 (2011), https://doi.org/10.1038/jid.2011.1.

[37] J. Chu, S. Jeffries, J.E. Norton, A.J. Capobianco, E.H. Bresnick, Repression of activator protein-1-mediated transcriptional activation by the notch-1 intracellular domain, J. Biol. Chem. 277 (2002), https://doi.org/10.1074/jbc.M111044200.
[38] J.W. Kim, M.J. Kim, K.J. Kim, H.J. Yun, J.S. Chae, S.G. Hwang, T.S. Chang, H. S. Park, K.W. Lee, P.L. Han, S.G. Cho, T.W. Kim, E.J. Choi, Notch interferes with the scaffold function of JNK-interacting protein 1 to inhibit the JNK signaling pathway, Proc. Natl. Acad. Sci. U. S. A. 102 (2005), https://doi.org/10.1073/pnas.0501600102.
[39] M.V. Giuli, E. Giuliani, I. Screpanti, D. Bellavia, S. Checquolo, Notch signaling activation as a hallmark for triple-negative breast cancer subtype, J. Oncol. 2019 (2019), https://doi.org/10.1155/2019/8707053.